NASA TECHNICAL TRANSLATION NASA TT F-16208

ELECTROCHEMICAL MEASUREMENTS IN MOLTEN NaOH

H. J. Krüger, A. Rahmel and W. Schwenk

Translation of "Elektrochemische Messungen in NaOH-Schmelzen," Electrochimica Acts, Vol. 13, 1968, pp. 625-643

NATIONAL AERONAUTICS AND SPACE ADMINISTRATION
WASHINGTON, D. C. 20545 APRIL 1975

STANDARD TITLE PAGE

1. Report No. NASA TT F-16208	2. Government Accession No.	3. Recipient's Catalog No.
4. Title and Subtitle ELECTROCHEMICAL MEASUREMENTS IN MOLTEN NaOH		5. Report Date April 1975 6. Performing Organization Code
7. Author(s) H. J. Kruger, A. Rahmel and W. Schwenk; Research Institute of Mannesmann AG, Duisberg, West Germany		8. Performing Organization Report No. 10. Work Unit No.
9. Performing Organization Name and Address Leo Kanner Associates Redwood City, California 94063		11. Contract or Grant No. NASw-2481 13. Type of Report and Period Covered Translation
12. Sponsoring Agency Name and Address National Aeronautics and Space Administration, Washington, D.C. 20546		14. Sponsoring Agency Code

15. Supplementary Notes Translation of "Elektrochemische Messungen in NaOH-Schmelzen," Electrochimica Acts, Vol. 13, 1968, pp. 625-643

16. Abstract Together with previous results, the electrochemical studies recorded in this article demonstrate that chemical processes, and not electrochemical ones, are rate-determining for the dissolution of metals and metal oxides in molten hydroxide. Chemical reaction between the melt and oxygen in the air forms peroxide, which is consumed in the corrosion reactions.

17. Key Words (Selected by Author(s))	18. Distribution Statement
	Unclassified-Unlimited

19. Security Classif. (of this report)	20. Security Classif. (of this page)	21. No. of Pages	22. Price
Unclassified	Unclassified	25	

ELECTROCHEMICAL MEASUREMENTS IN MOLTEN NaOH

H. J. Krüger, A. Rahmel and W. Schwenk
Research Institute of Mannesmann AG,
Duisberg, West Germany

Abstract -- A thermodynamic discussion of the Pt/O_2 electrode in molten NaOH shows that the redox potential depends on P_{O_2}, P_{H_2O}, $a_{O_2^{2-}}$ and $a_{O^{2-}}$. Potential measurements have shown that the reaction $O_2 + 2e^- = O_2^{2-}$ determines the potential. Of all the electrode materials investigated -- Pt, Au, Ag, Ni and Fe -- only the last one exhibits a positive potential shift relative to the other metals; this shift has been ascribed to O_2^{2-} depletion following corrosion.

The peroxide required for the corrosion reactions can be formed only by chemical reaction of the melt with O_2, but not by anodic oxidation, since peroxide oxidation essentially precedes the oxidation of hydroxide ions to oxygen and water vapor. In both anodic and cathodic polarization, peroxide reaction and generates limiting currents, the anodic reation being less inhibited. Water vapor is reduced cathodically, generating limiting currents, before NaOH is reduced to H_2 and OH^-. Anodically, Pt corrosion is stimulated by water vapor, producing current fluctuations. In pure molten NaOH, the cathodic reduction may be assumed to be the formation of H_2 and Na_2O, and not Na deposition.

/625*

Introduction

/626

Along with studies on the corrosion of certain metals and oxides in molten NaOH [1], electrochemical experiments were also conducted in these melts, and the results will now be reported. The objective of these studies was to gain somewhat more insight

* Numbers in the margin indicate pagination in the foreign text.

into the reactions occurring when steels are pickled in molten NaOH, particularly in the so-called "Hooker Bath".

The electrochemical properties of metals and oxides in molten NaOH has not been studied very much. Neumann and Bergve [2] electrolyzed mixtures of molten KOH and NaOH. Agar and Bowden [3] studied the evolution of oxygen on nickel and platinum electrodes at 340° C. Stern and Carlton [4] measured potentials on silver, copper, nickel, cobalt, and tungsten between 340 and 600° C. Kern and co-workers [5,6] recorded current-density/potential curves and found that there were limiting currents in the cathode area, depending on the water content of the melt, and that these currents were due to cathodic reduction of the water. The most comprehensive studies were conducted by Goret [7] on eutectic melts of NaOH and KOH at 220° C. Current-density/potential curves were recorded for platinum, gold, and nickel. Limiting currents observed in the cathode area were likewise attributed to the reduction of the water in the melt. Also, the reduction of peroxide added were formed from oxygen yielded limiting currents proportional to the peroxide content.

The problem of a reference electrode stable in alkali hydroxide has not yet been satisfactorily resolved. Because of the great aggressivity of these media, glasses and other materials containing SiO_2 cannot be used, since they corrode very rapidly. For this reason, in the few studies conducted so far, the reference electrode is often just an inert precious-metal-wire electrode dipped into the melt [3,4]. As will be shown, constant experimental conditions usually give rise to potentials which are quite constant in time. At the same time, proposals have been made for a reference electrode in molten alkali hydroxides. Rose, Davis and Ellingham [8] used an oxygen electrode with silver or platinum wire to measure the enthalpy of formation of SnO_2 and PbO in NaOH between 400 and 700° C. Kern and co-workers [5,6] gave two reference electrodes in succession. The first consisted of a palladium tube closed at one end, with internal hydrogen circulation. Because of the solubility of

hydrogen in palladium, this electrode was said to be based on the H_2/H_2O equilibrium in the melt. However, the system did not work quite satisfactorily, since any change in the water content of the melt influenced the equilibrium potential. The second reference electrode developed for this reason was a metal/metal-oxide electrode and was based on the solubility of Au_2O_3 in molten alkali hydroxide. To make it, gold was dissolved anodically until the maximum solubility was reached. The melt was placed in an alumina tube, closed at one end with a porous graphite stopper, and the gold wire immersed in it. The electrode was said to be usable between 200 and 500° C, and quite insensitive to changes in the gas atmosphere.

Theoretical Foundations of the Redox Potential

In the present experiments, a Pt/O_2 electrode was studied with the following concentration chain:

$$Pt(O_2/H_2O)/NaOH,\ O^{2-}\ or.\ O_2^{2-}/NaOH,\ O^{2-}\ or.\ O_2^{2-}/Pt(O_2/H_2O).$$

The crucial factor in determining the potential may be the /627
reduction of oxygen to the oxide anion

$$O_2 + 4e^- = 2\ O^{2-}. \tag{1}$$

However, since Lux and Niedermaier [10, 11] state that molten NaOH containing oxygen exhibits considerable concentrations of peroxide, a stepwise reduction of the oxygen must also be considered. These electrode reactions

$$O_2 + 2e^- = O_2^{2-} \tag{2}$$

$$O_2^{2-} + 2e^- = 2\ O^{2-} \tag{3}$$

obey the Nernst equations

(a) for (1)
$$E_1 = E_1^\circ - \frac{RT}{4F} \ln \frac{a_{O^{2-}}^2}{p_{O_2}}, \tag{4}$$

(b) for (2)
$$E_2 = E_2^\circ - \frac{RT}{2F} \ln \frac{a_{O_2^{2-}}}{p_{O_2}}, \tag{5}$$

(c) for (3)
$$E_3 = E_3^\circ - \frac{RT}{2F} \ln \frac{a_{O^{2-}}^2}{a_{O_2^{2-}}}. \tag{6}$$

The chemical reactions in the melt can be described by the following equations

$$H_2O + O^{2-} = 2\ OH^-, \tag{7}$$

with

$$K_7 = \frac{1}{a_{O^{2-}} \cdot p_{H_2O}}, \tag{8}$$

$$O_2^{2-} + H_2O = 2\ OH^- + \tfrac{1}{2}O_2, \tag{9}$$

with

$$K_9 = \frac{p_{O_2}^{1/2}}{a_{O_2^{2-}} \cdot p_{H_2O}}. \tag{10}$$

In (8) and (10), a_{OH^-} is assumed to be constant. We also presume that the phase equilibria

$$\mu_{H_2O}^{melt} = \mu_{H_2O}^{gas} \tag{11}$$

and

$$\mu_{O_2}^{melt} = \mu_{O_2}^{gas} \tag{12}$$

are reached, so that the activities a_{H_2O} or a_{O_2} can be replaced by the partial pressures p_{H_2O} or p_{O_2}.

Through reactions (7) and (9), the four variables p_{O_2}, p_{H_2O}, $a_{O^{2-}}$, and $a_{O_2^{2-}}$ are in equilibrium. Except for the combination of variables ($a_{O^{2-}}$, p_{H_2O}), fixing any two of the variables determines the other two. This yields a total of $\binom{4}{2} - 1 = 5$ possible combinations. In equilibrium, all three electrode reactions (1), (2), and (3) have the the same potential, which obeys e.g. the equation (13), derived as a function of p_{H_2O} and p_{O_2}. However, this can also be given as a function of anyone of these five variable combinations ($a_{O^{2-}}$, p_{O_2}), ($a_{O_2^{2-}}$, p_{O_2}), ($a_{O_2^{2-}}$, p_{H_2O}), and ($a_{O_2^{2-}}$, $a_{O^{2-}}$). /628

$$E = E^+ + \frac{RT}{4F} \ln p_{O_2} + \frac{RT}{2F} \ln p_{H_2O}. \tag{13}$$

Because of this dependence of the redox potential of the molten NaOH on the partial pressures of oxygen and water vapor, a reference potential could be established. The reference was chosen to be the potential obtained for platinum in NaOH under p_{O_2} = 0.98 atm and p_{H_2O} = 0.02 atm. With the aid of (13), all measured potentials were converted to this reference point, so that in most of the experiments, the reference electrode did not require its own electrode space. It is easy to obtain the water-vapor partial pressure of 0.02 atm experimentally, since the corresponding dew point is 17.7° C.

Apparatus and Execution

The organization of the experiment can be seen in Fig. 1. The actual reaction chamber in the interior of the furnace is formed by a nickel pipe welded to the base. Nickel was chosen to be the material for the reaction vessel, since it is quite resistant to vapors from NaOH and also to overflowing NaOH melt if there are leaks in the crucibles. The upper end of the nickel pipe was sealed with a vacuum-type flange joint. The guide tubes for the electrodes and a thermocouple were four pipes of 18/8 chromium-nickel steel, projecting 10 cm into the reaction chamber, and hard soldered to the cover by gas-tight joints. The gas intake tube was attached in the same fashion. Just below the upper end of the pipe, a connection for allowing gas to escape or for hooking up a vacuum pump was welded on. Above the support plate, the pipe was cooled by water flowing through a copper coil. The furnace temperature was regulated largely by hand, utilizing constant voltage. The temperature, measured by a Pt/Pt-Rh thermocouple immersed in the melt, usually fluctuated by less ± 2° C. Because of the aggressive nature of the melt, we did not bother with a protective jacket for the thermocouple. Most of the experiments were conducted in cylindrical crucibles of fine silver 0.5 mm thick, 41 mm in diameter (exterior), and 50 mm tall. A platinum crucible or a crucible of pure alumina was used in isolated cases. As a rule, the melt sat under the reaction gas for about 2 hours before measurements began, in order to permit melt/gas equilibration to occur.

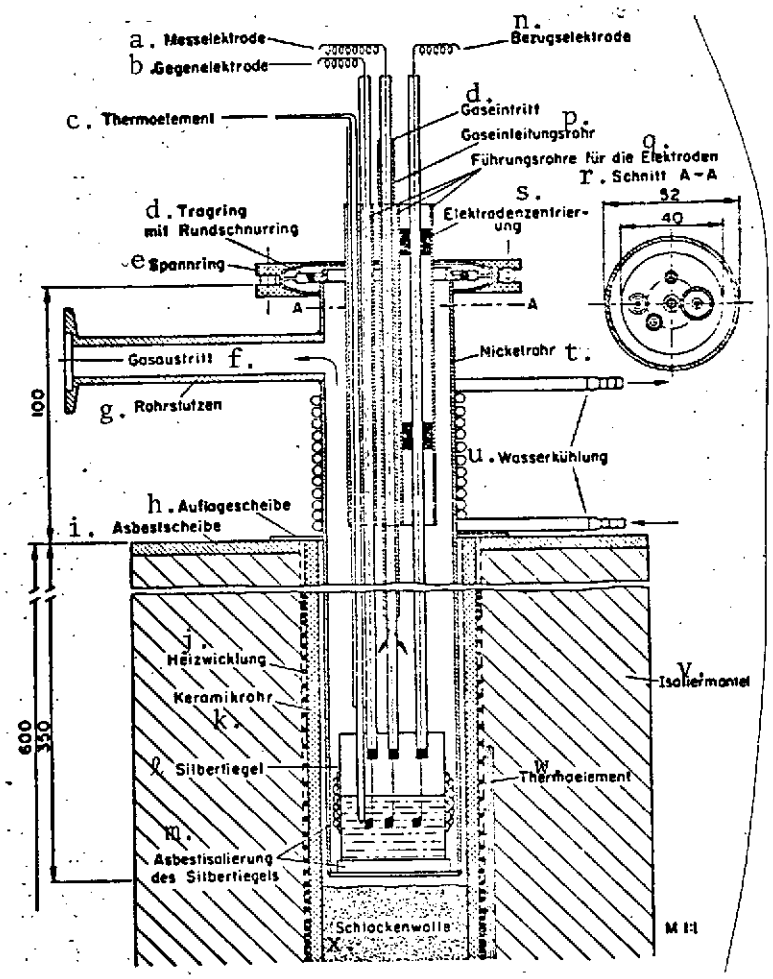

Fig. 1: Apparatus

Key:
a. measuring electrode
b. counter electrode
c. thermocouple
d. mantle ring with O-seal
e. set screw ring
f. escaping gas
g. pipe connection
h. support plate
i. asbestos disc
j. heating coil
k. ceramic pipe
l. silver crucible
m. asbestos insulation of silver crucible
n. reference electrode
o. gas inlet
p. gas intake pipe
q. guide tubes for electrodes
r. section
s. electrode centering unit
t. nickel pipe
u. water cooling
v. insulating jacket
w. thermocouple
x. slag wall

Because of the aggressive nature of the molten NaOH, the design and arrangement of the electrodes raised numerous problems. The best electrode holder proved to be a pure nickel tube 0.5 mm thick, 3.5 mm in diameter (exterior), and 555 mm long. At one end of the tube, a pure nickel cylindrical stopper 3 mm long was inserted and welded in a gas-type seal to the tube. Then a platinum wire 0.5 mm in diameter was drawn through the tube and through a 0.6 mm hole in the stopper. The tube was then scaled for 40-50 h at 1180° C in air, oxygen being introduced into the pipe during the first 10 hours to promote oxidation. Oxidation of the nickel embedded the platinum /629
wire in the stopper, and insulated the wire from the metallic nickel by a dense nickel-oxide layer of high electrical resistance. After the oxidation, a check was made to ensure that there were no leaks around the platinum wire. Also, the resistance between the nickel pipe and the platinum wire was measured. At room temperature, the resistance was greater than $10^6\Omega$, while it was about one order of magnitude lower at 500° C. After each test, the electrodes were washed free of alkali using distilled water, the closed end of the pipe and the platinum wire were annealed for a short time, and the resistance measurement was repeated.

In the experiments involving pure nickel and pure iron, 0.15 mm thick metal strips were welded to the platinum wire of the electrode. The 20 mm long strips were immersed about half way into the melt. The surface of the specimans was about 1.3 cm^2. Almost all the electrochemical tests were carried out with these electrodes, the essential feature of which was the platinum wire being held in the nickel pipe by the oxide. In this form, the electrodes could serve as reference electrodes, counter electrodes, or measuring electrodes.

Experiments on the effect of the partial pressures of oxygen /630
where water vapor on the redox potential of NaOH, the platinum electrodes were passed through alumina tubes 1.5 mm thick, 8 mm in diameter (exterior) and 545 mm long. Gases were introduced through these tubes. The alumina tubes used to separate the electrode

spaces had a 0.5 mm hole in the lower closed end, so that there was an electrolyte bridge between the two electrodes across the melt in the crucible.

In experiments on the change in redox potential due to addition of salts, the electrode space for the molten NaOH without additives (reference electrode) was a short piece of pipe, closed at one end, made of aluminum oxide, 2.5 mm thick, 17 mm in diameter (exterior), and 60 mm long. There was a hole 1 mm in diameter about halfway up the pipe (about 10 mm above the melt in the crucible). The electrolytic connection between the melts in the crucible and in the pipe was produced by molten NaOH climbing the pipe.

The potential was measured without capillary probes. The measured value was off by the ohmic voltage drop in the electrolyte. However, this error was small because of the high specific electrical conductivity of molten NaOH -- e.g. 0.303 $\Omega \cdot$ cm at 450° C [9]. An estimate indicated that the voltage drop should be < 0.5 mV/mA. The degree of purity of the fine gold, fine silver, and chemically pure platinum was 99.98%. The pure iron melted in vacuum contained > 99.9% Fe as well as 0.028% N and 0.02% each Mn and Si. The other impurities were < 0.01%. The 2 mm nickel sheet contained 99.8% Ni and a maximum of 0.02% of any other element, according to the figures of the manufactuer. The NaOH employed (analytical grade) was in the form of plates according to our analysis, it contained 0.2% Na_2CO_3 and about 0.7% H_2O. The substances Na_2CO_3, $NaNO_3$, $NaNO_2$ and Na_2O_2 were analytical grade. The Na_2O was 98% pure. Oxygen with 99.9% purity, nitrogen with 99.99% purity, or mixtures of these gases with 1 or 10% O_2 were employed. The water vapor content was < 100 ppm leaving the bottle and 150-250 ppm leaving the apparatus. To achieve specific partial pressures of water vapor, the gas was passed through three successive thermostatic washing bottles filled with distilled water.

Experimental Results

(a) Measurement of Redox Potential

In the experiments on the influence of the oxygen partial pressure, p_{H_2O} = constant. For 500° C, (13) gives the following value after numerical values have substituted for R, F, and T:

$$\left(\frac{\partial E}{\partial \ln p_{O_2}}\right)_{p_{H_2O}} = 0.0383 \text{ V.} \qquad (14)$$

Fig. 2 shows that the experimental values lie very close to the theoretical line with the fault given by (14). In the experiments on the influence of the water vapor partial pressure, p_{O_2} = constant. For 500° C, (13) gives

$$\left(\frac{\partial E}{\partial \ln p_{H_2O}}\right)_{p_{O_2}} = 0.0765 \text{ V.} \qquad (15)$$

For 400° C, this quotient is 66.7 mV. Fig. 3 shows that the experimental values for 400 and 500° C agree well (15). The slope is independent of whether oxygen or nitrogen is used as the carrier /631 gas for the water vapor. The difference of 155 mV between the parallel lines for oxygen and nitrogen corresponds to an oxygen content of about 0.01% in the nitrogen.

Fig. 4 gives potential vs. time for platinum in NaOH under oxygen as the partial pressure of the water vapor is varied. Equilibration between the melt and the reaction gas is much faster when the water vapor pressure is raised than when it is lowered. Under nitrogen, the situation is precisely reversed.

Since the thermodynamic analysis does not show which reaction determines the potential, we next investigated non-equilibrium states, in which oxide or peroxide is added to the molten NaOH with constant gas flow.

Increasing the oxide ion concentration in the melt by adding Na_2O hardly changed the potential at all under both oxygen and

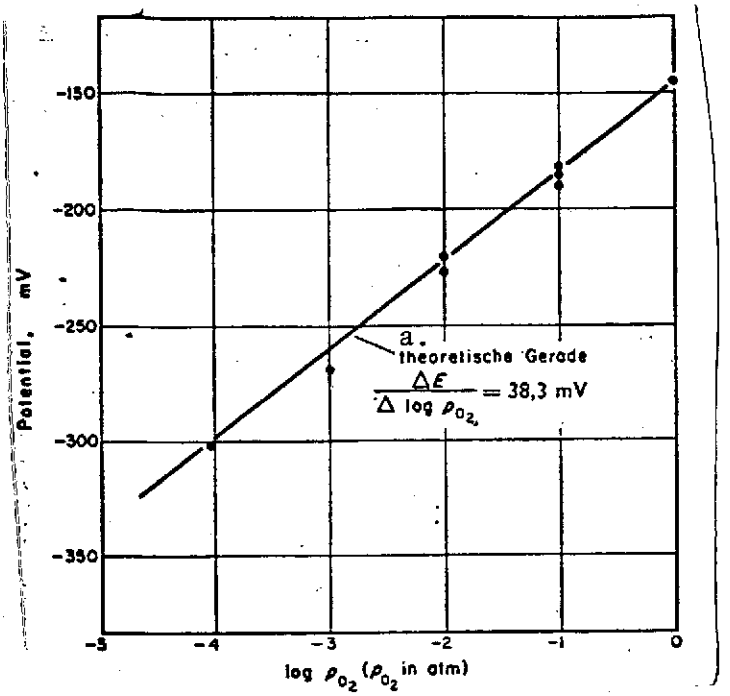

Fig. 2: Influence of O_2 pressure on potential of Pt/O_2 electrode in NaOH at 500° C. (water vapor content = 0.025%).

Key: a. theoretical line

nitrogen. According to (4), the fact that the potential is independent of Na_2O addition means that the electrode reaction (1) is not potential-determining. It can also be deduced that an electrode reaction corresponding to (13) and obtained by combining (1) and (7), i.e.

$$O_2 + 2\ H_2O + 4e^- = 4\ OH^- \quad (16)$$

cannot be potential-determining either. This does assume, however, that reaction (7) takes place fast enough, and that Na_2O is dissociated into Na^+ and O^{2-} ions.

Adding Na_2O_2 yielded a clear connection between potential and peroxide concentration in the melt under both oxygen and nitrogen. The results are shown in Fig. 5. With the usual pre-melting time of 2 hours under nitrogen (curve a) and under oxygen (curve b), the following relation is obtained

/633

$$E = K - \frac{RT}{2F} \ln c, \quad (17)$$

where c is the concentration of peroxide ion added in wt-%. This equation corresponds to (5) at constant p_{O_2}. Substituting the numerical values for R, T, and F supplies

$$E = E^\circ - 0{,}0765 \log \frac{c}{p_{O_2}}, \quad (17a)$$

$$E = K(p_{O_2}) - 0.0765 \log c. \quad (17b)$$

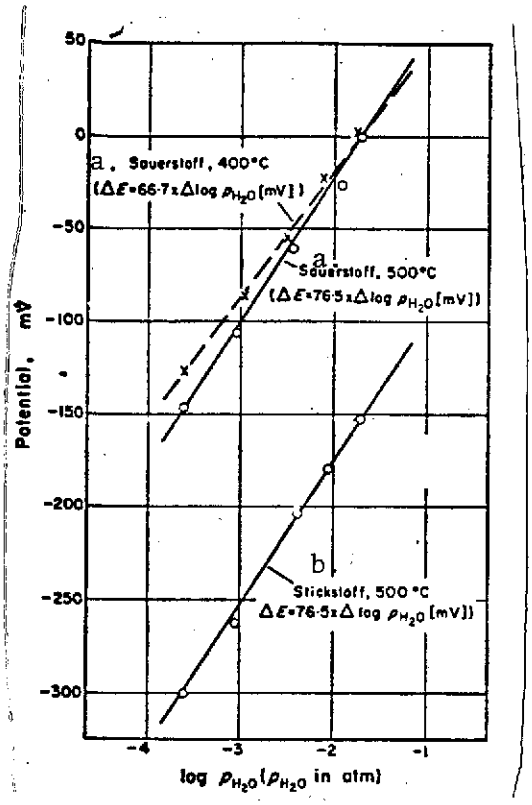

Fig. 3: Influence of H_2O pressure on potential of Pt/O_2 electrode in NaOH at 400 and 500° C (solid lines = theoretical lines).

Key: a. oxygen
b. nitrogen

This equation corresponds to the solid lines in Fig. 5. This result implies that electrode reations (2), i.e. reduction of oxygen to peroxide ion, takes place rapidly and is therefore potential-determining.

Electrode reation (3) cannot be potential-determining for the following reasons. At constant oxygen pressure, the oxide ion concentration is proportional to the peroxide concentration, as indicated by combining (7) and (9): /634

$$O_2^{2-} = O^{2-} + 1/2\ O_2. \qquad (18)$$

If this equilibrium were reached rapidly, the potential would have to be independent of any addition of either oxide or peroxide, if the electrode reaction (3) were potential-determining. If the equilibrium (18) were reached very slowly, the potential would be changed by adding either oxide or peroxide. Both possibilities conflict with the measurements.

Equation (17) contains the assumption that the peroxide concentrations c_o present before the addition was small in comparison with the added peroxide c. Otherwise, the equation would have to read

$$E = K - \frac{RT}{2F} \ln (c_0 + c). \qquad (19)$$

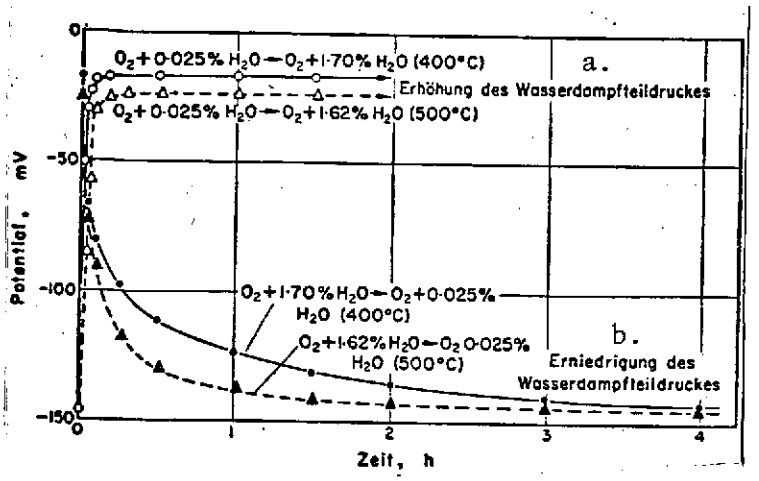

Fig. 4: Equilibration of potential of Pt electrode after changing H_2O partial pressure in O_2 at 400 and 500° C.

Key: a. raising partial pressure of water vapor
b. lowering partial pressure of water vapor

The curve for function (19) has two branches in a simple logarithmic coordinate system. The asymptotes correspond to the equations

$$E = E_0 - \left(\frac{RT}{2F}\right) \ln 10 \cdot \log c_0 \text{ for } c \ll c_0, \quad (19a)$$

$$E = E_0 - \left(\frac{RT}{2F}\right) \ln 10 \cdot \log c \text{ for } c \gg c_0. \quad (19b)$$

The first line is parallel to the horizontal axis and describes the potential for zero peroxide addition. The intersection of the two lines has the coordinates E_0, c_0. The initial concentration c_0 can be found in this way. In accordance with Fig. 5, we find c_0 = 0.028 wt-% under oxygen, and 0.029 wt-% O_2^{2-} under nitrogen. The low peroxide content of the melt under oxygen appears to contradict the statements of Lux and coworkers [11]. However, this can be explained by supposing that the equilibrium (9) between peroxide and oxygen is not achieved in the relatively short time of two hours. Therefore, experiments were conducted in which the molten NaOH was held 29 hours under oxygen with differing flow rates, before the peroxide was added. As Fig. 5 shows, the influence of identical peroxide doses on the redox potential diminishes with increasing oxygen flow rate during the premelting period, so that peroxide formation increases with rising flow rate during the premelting period.

The initial concentration of peroxide can be calculated with the aid of (19)

$$\Delta E = E_{(c+c_0)} - E_{(c_0)} = -\frac{RT}{2F} \ln\left(\frac{c}{c_0} + 1\right) \quad (20)$$

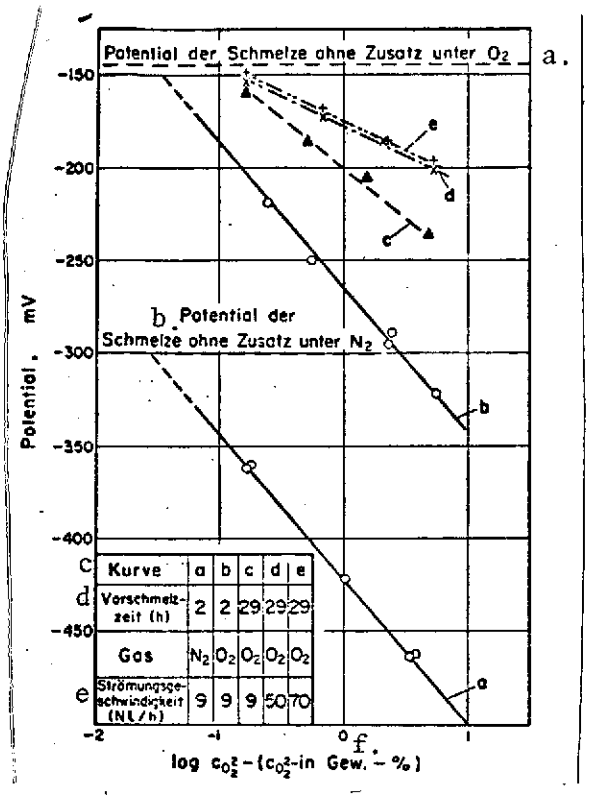

Fig. 5: Influence of Na_2O_2 addition on potential Pt electrode in NaOH at 500° C.

Key: a. potential of melt without addition under O_2
b. potential of melt without addition under N_2
c. curve
d. pre-melting time
e. flow rate
f. wt-percent

with

$$c_0 = \frac{c}{\exp\left(-\frac{\Delta E}{33.3}\right) - 1} \cdot \qquad (21)$$

If ΔE is replaced by the experimental values for a peroxide dose c of 1.60 wt-%, flow rates of 9, 50, and 70 standard ℓ O_2/h yielded initial peroxide concentrations c_0 of 2.16, 2.80, and 3.20 wt-% after 29 hours. These values are quite close to those of Lux and co-workers [11], namely 3.5-5 wt-%. /635

The influence of some other sodium salts was studied at 500° C under oxygen and nitrogen. Adding the salts Na_2CO_3, $NaNO_2$, $NaNO_3$, Na_2CrO_4, $Na_2Cr_2O_7$, $Na_2B_4O_7$, and $NaAlO_2$, which are present in the "Hooker Bath", caused virtually no change in the potential.

(b) Measurement of Rest Potential for Platinum, Gold, Silver, Nickel and Iron

Rest potential vs. time was measured for various metals under pure oxygen, under nitrogen with 1-10 vol-% oxygen, and under pure nitrogen. Regardless of the atmosphere, virtually identical rest potentials were obtained for gold and silver, shifted by + 7 ± 1 mV relative to that of platinum. As the oxygen partial pressure was reduced, it took longer and longer for the constant rest potential to be reached. This tendency was more distinct for gold than for silver. Rest potential vs. time is plotted in

Fig. 6 for iron and nickel. At the beginning, the potentials were more negative than the steady-state values. While the potential of nickel was practically the same as that of platinum, iron exhibited a potential up to 55 mV more positive than platinum. This difference became smaller as oxygen partial pressure decreased. Decreasing the oxygen content of the atmosphere made the rest potentials of iron and nickel less reproducible and more negative than those of gold and silver. Just after insertion, potentials between -500 to -600 mV were measured for iron and between -700 to -800 mV for nickel, relative to platinum. The nickel specimens remained metallically shiny in brief experiments.

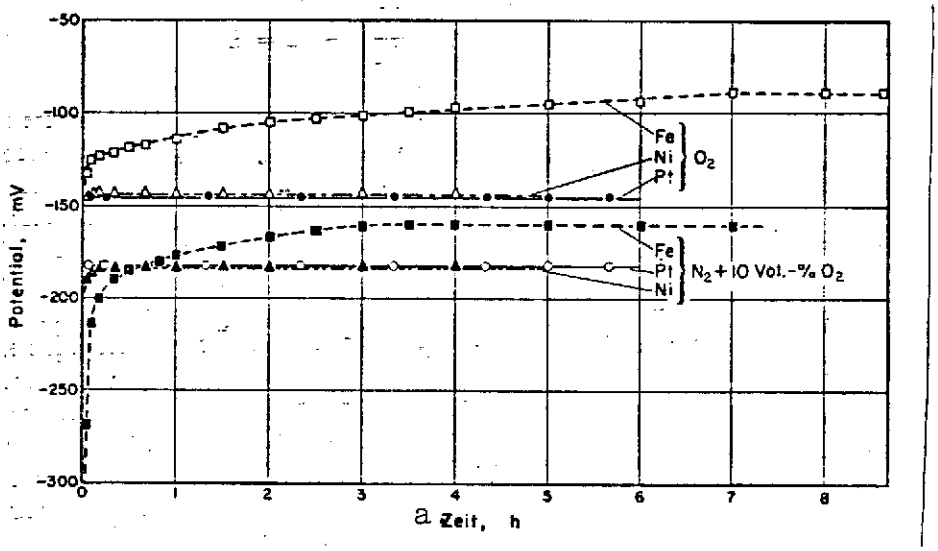

Fig. 6: Rest potential of Pt, Ni, and Fe vs. time in different gases. [Key: a. time]

(c) Galvanostatic Studies on Platinum, Gold, and Silver in NaOH, $NaNO_3$, and a Mixture of These Salts.

The results of galvanostatic polarization measurements are shown in Fig. 7, 8, and 9. For silver, the current-density/potential curve under oxygen and nitrogen with 1% O_2 are almost parallel (Fig. 7). Fig. 8 shows the current-density/potential curves for silver, platinum, and gold in NaOH under oxygen at 600° C. The curves /637

were independent of whether they were measured with rising or falling current densities. The polarize ability of metals increases slightly in the sequence named, the cathodic polarizability being somewhat less than the anodic in every case. Adding nitrates had virtually no influence on the current-density/potential curves in NaOH for silver. On the other hand, the polarizability in pure $NaNO_3$ is very large (Fig. 9).

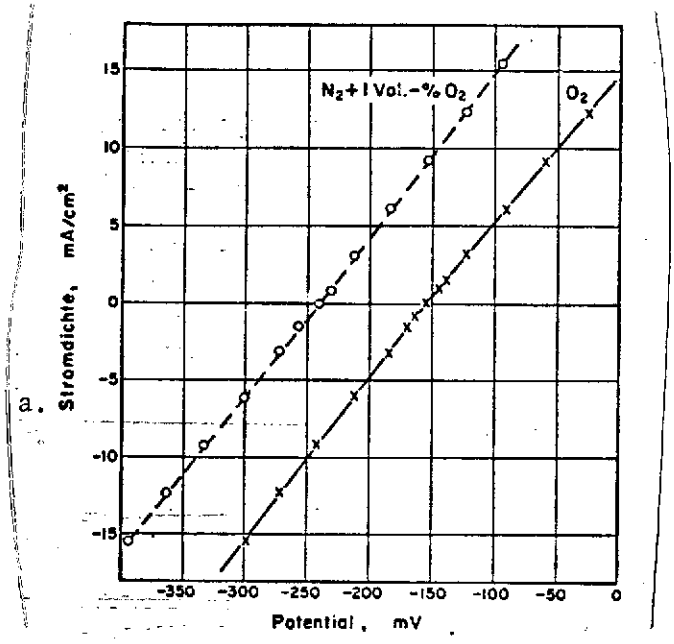

Fig. 7: Galvanostatic current-density/potential curves for Ag under O_2 and N_2 with 1% O_2.

Key: a. current density

In the galvanostatic circuit, the Faraday yield of silver in NaOH under nitrogen at 400 and 600° C was determined gravimetrically as the function of current density. With increasing current density and falling temperature, the current yield decreases (Fig. 10). A cathodic redox current was ignored in calculating the Faraday yield, since the corrosion rate was negligible relative to anodic dissociation even at the rest potential. Fig. 11 shows the galvanostatically determined anodic curves for the current and for the branch current of silver dissociation. The mass loss of the silver anode usually agrees with the silver content of the melt. The filtrate of the solution contained no silver [1]. Often, part of the dissolved silver had deposited on the cathode. Corresponding experiments for platinum and gold show that the Faraday yields increase in the sequence platinum-gold-silver.

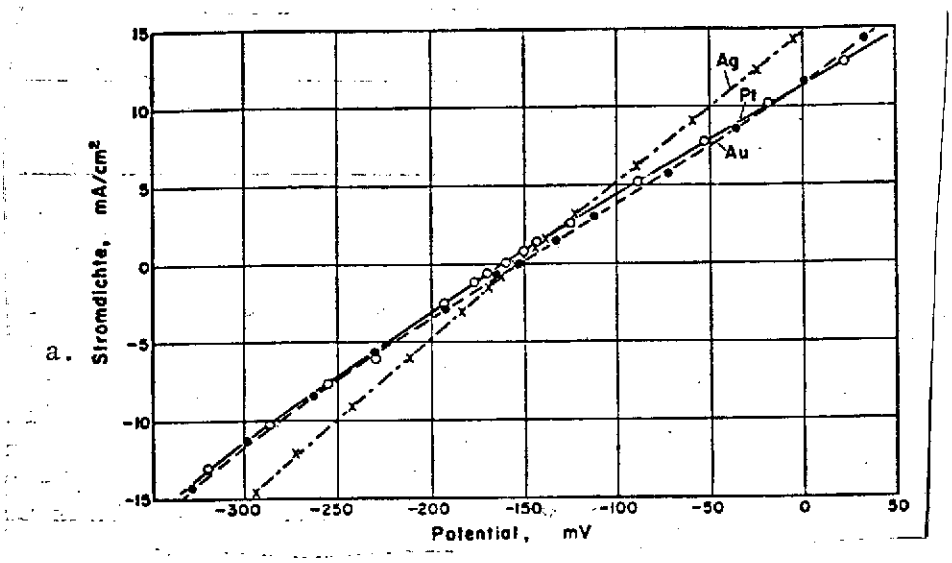

Fig. 8: Galvanostatic current-density/potential curves for Pt, Au and Ag under O_2 at 600° C.

Key: a. current density

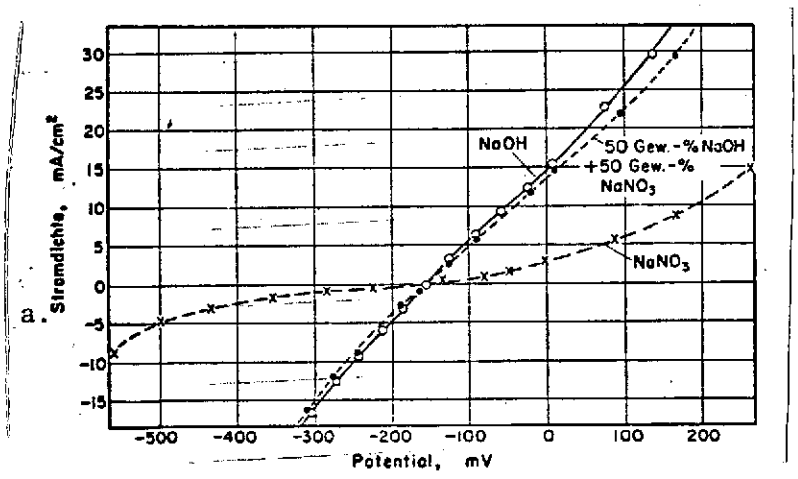

Fig. 9: Galvanostatic curren-density/potential curves for Ag in NaOH, $NaNO_3$, and a mixture of the two salts under O_2 at 600° C.

Key: a. current density
gew.-% = wt-%

(d) Potentiostatic Polarization Measurements for Platinum, Iron and Nickel

In potentiostatic holding experiments under various gases at 500° C, a steady current was obtained after a few minutes. Fig. 12 shows the potentiostatically recorded current-density/potential curves for platinum, iron, and nickel under nitrogen and nitrogen with 10 vol-% oxygen. Under nitrogen, platinum is very polarizable both anodically and cathodically. Anodically,

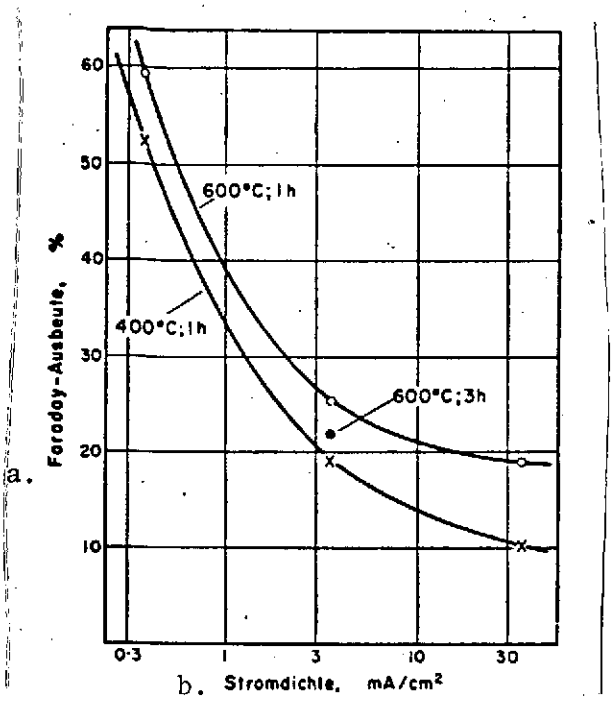

Fig. 10: Influence of current density on Faraday yield for Ag dissolving in NaOH at the anode, under O_2 at 400 and 600° C.

Key: a. Faraday yield
b. current density

the current rises very rapidly, starting at about + 0.8 V. In this case, it is obvious that hydroxide ions are being oxidized

$$2\ OH^- = H_2O + 1/2O_2 + 2e^-. \qquad (22)$$

Cathodic polarization yielded very slight current densities at potentials through about - 1.3 V. The subsequent current rise may be attributed either to the reduction of sodium ions

/639

$$2\ Na^+ + 2e^- = 2\ Na \qquad (23)$$

or to the reduction of hydroxide ions

$$2\ OH^- + 2e^- = 2\ O^{2-} + H_2. \qquad (24)$$

In the experiments under nitrogen with 10 vol-% oxygen, a current rise was measured at just -0.1 V, in this case, the electrode reaction (22) must be preceded by another reaction associated with the formation of peroxide under an atmosphere containing oxygen. The cathode current density vs. potential curves under nitrogen with 10 vol-% oxygen are shifted toward higher current densities by comparison with the curves under pure nitrogen. From about -0.5 V, a limiting current is developed around -15 mA/cm².

The current density vs. potential curves for iron and nickel under N_2 + 10% O_2 differ only slightly from those for platinum. Under pure nitrogen, on the other hand, somewhat greater discrepancies are observed. In the cathode area, the curves for nickel and platinum practically coincide, while the current density for iron is about an order of magnitude greater. In the anode area, the curves for iron and nickel are lower than that for platinum.

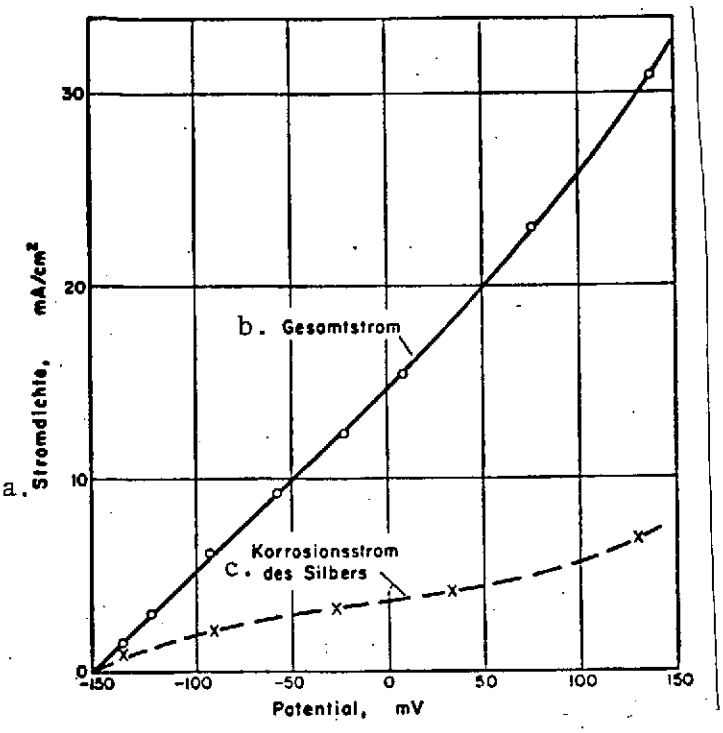

Fig. 11: Galvanostatically measured current-density/potential curves for Ag under O_2 at 600° C.

Key: a. current density
b. total current
c. corrosion current of silver

Since potentiostatically recorded current density vs. potential curves for platinum agree with the corresponding curves recorded with potential varying by 2 V/h, the remaining experiments were conducted potentiokinetically. Fig. 13 shows current density vs. potential curves for platinum under nitrogen with Na_2O_2 added. It can be seen that adding peroxide has the same effect on the curves as raising the partial pressure of oxygen. Adding slight quantities, less than 1 wt-%, has practically no effect. The cathode limiting current densities increase with the peroxide content of the melt. Also, measurements using platinum were conducted under mixtures of nitrogen and water vapor (Fig. 14). The cathode curves show a current rise at about -1.2 V and finally the formation of limiting currents, which increase with rising water vapor content. The drop in current density observed with falling potential may be due to depletion of water in the cathode area in all experiments. The further current rise at about -1.8 V can be attributed to the reaction in either equation (23) or (24). /641

In the anode area, the current already begins to rise at about + 0.2 V under nitrogen containing water vapor. After a short steady curve region, current fluctuations appear. The onset of

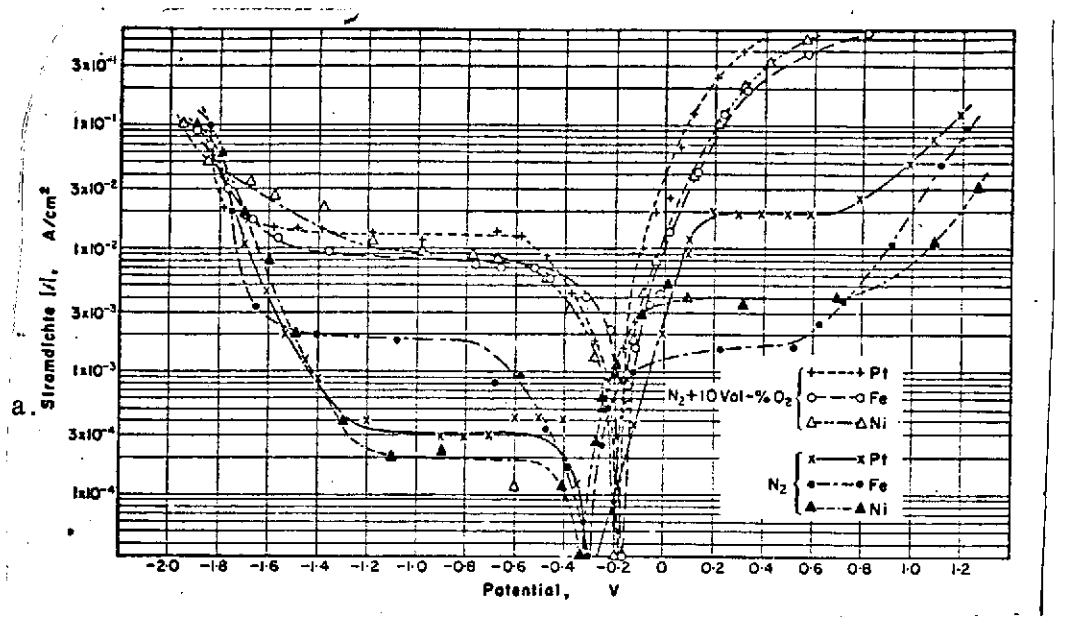

Fig. 12: Potentiostically measured current density vs. potential curves for Pt, Ni and Fe under N_2 and 90% N_2 + 10% O_2 at 500° C.

Key: a. current density

these fluctuations is shifted toward higher potentials and currents as the water vapor content is increased. These current fluctuations may be due to water vapor increasing the dissociation of the platinum, followed by unstable passivity. A supporting fact is that one-hour static-potential holding experiments at + 0.3 V under nitrogen with water vapor yielded more platinum or platinum oxide in the melt then was found in an experiment under dry nitrogen.

Discussion of Results

Thermodynamic analyses on the Pt/O_2 electrode in molten NaOH show that the redox potential is a function of p_{H_2O} and P_{O_2} and of four other combinations of variables with the activities of O_2^{2-} and O^{2-}. It has been shown experimentally that of the three possible electrode reactions, the reduction of O_2 to O_2^{2-} takes place fast, and is thus potential-determining.

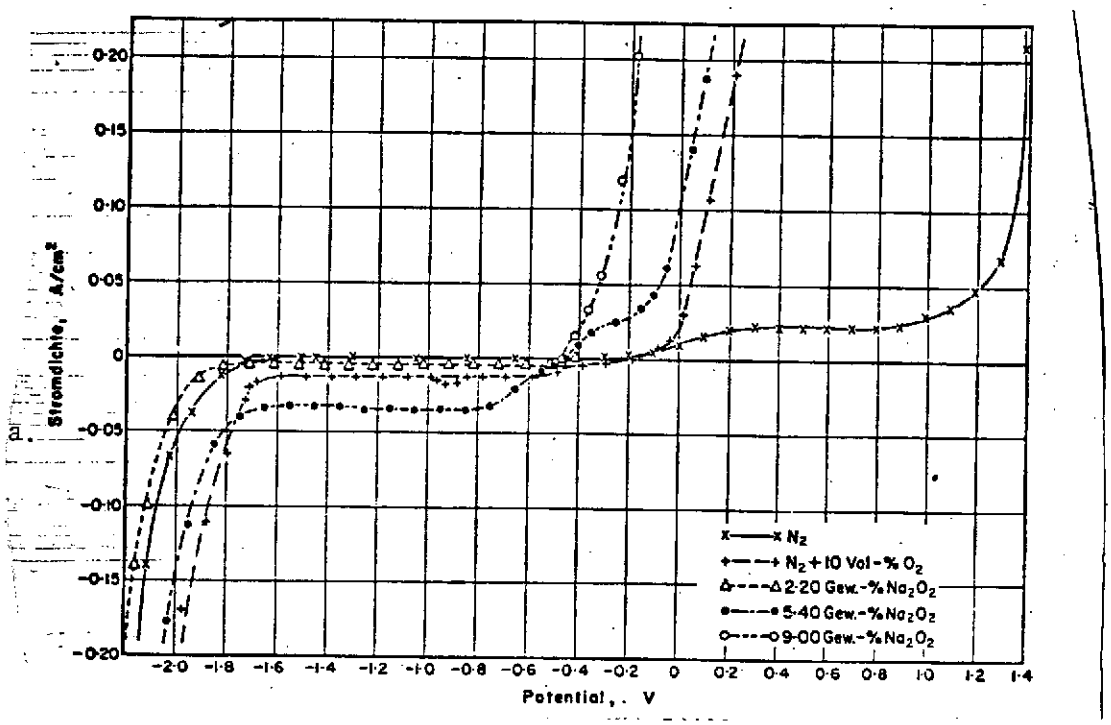

Fig. 13: Influence of gas composition and addition of Na_2O_2 on current density vs. potential curve for Pt at 500° C (potential varying at 2 V/h).

Key: a. current density
Gew.-% = wt-%

Potential equilibration when the gas atmosphere is changed depends essentially on peroxide formation and decomposition in accordance with (9). In agreement with Lux and Niedermaier [10], it was found that equilibration is faster in a moist atmosphere than in dry oxygen (Fig. 4). In oxygen, the removal of the resulting water is also decisive. Accordingly, the rate of formation of peroxide increases when the flow rate is raised. Compare Fig. 5 in connection with (21).

From the effects of adding peroxide on the redox potential, particularly under nitrogen, it can be inferred that the thermal decomposition of the peroxide in accordance with (18) is still strongly inhibited at 500° C. Since Nernst's equation (17) has been confirmed experimentally, the concentration and activity of the peroxide must be proportional, i.e. the degree of dissociation is constant.

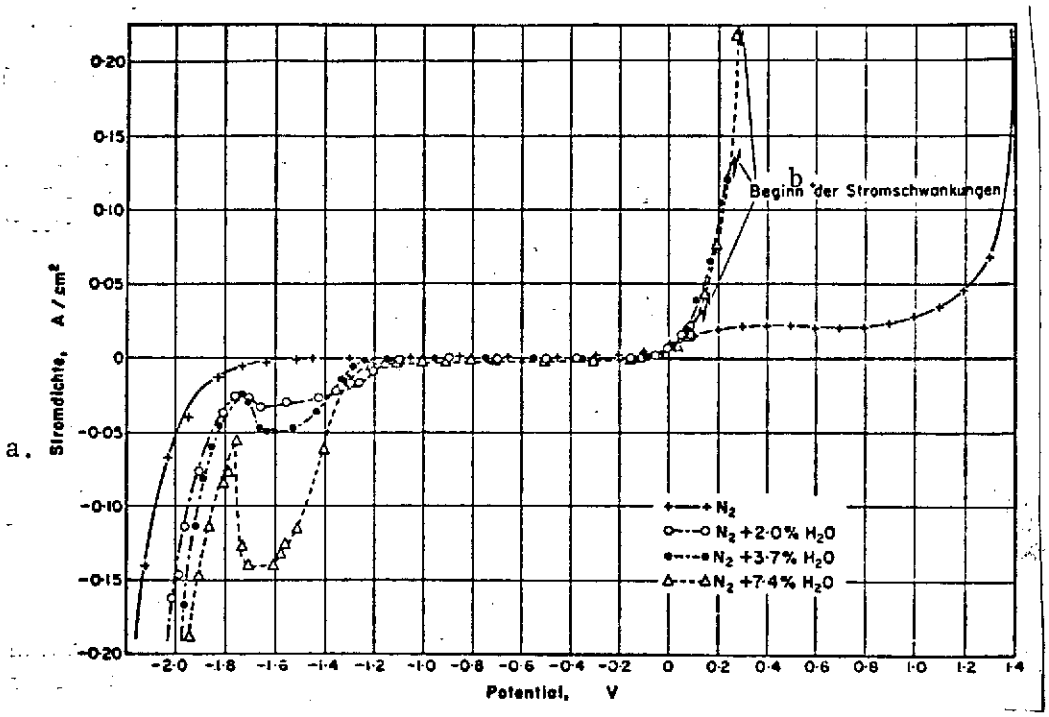

Fig. 14: Influence of H_2O partial pressure in N_2 on current density vs. potential curve for Pt at 500° C (measured potentiokinetically with 2 V/h).

Key: a. current density
b. onset of current fluctuations

The rest potentials measured for the metals Pt, Ag, Au, Ni, and Fe are probably not genuine redox potentials of the melt, but mixed potentials caused by corrosion of the metal. Since this corrosion is very slight with e.g. Pt and Au, and since the rest potentials under dry nitrogen-containing gases are identical, with the exception of Fe, the mixed potentials may coincide with the redox potentials. The shift in the rest potential of Fe (see Fig. 6) can be interpreted as peroxide depletion in the melt as a result of iron corrosion. Corrosion of iron is more than an order of magnitude greater than that of the other metals [1]. Since peroxide formation is inhibited in accordance with (9), peroxide depletion can develop and thus raise the potential in accordance with (17). The initial potentials for bare Ni and Fe electrodes observed under nitrogen- /642
free gases were considerably more negative than those for Pt and

can be interpreted, in agreement with Stern and Carlton [12], by corrosion resulting in a covering layer. Traces of nitrogen are sufficient to produce this covering layer and to bring the potential to the Pt value [12, 13]. The negative initial potentials under nitrogen provide an explanation for the fact that under these conditions, silver deposits were found in corrosion tests in silver crucibles with Fe and Ni [1].

Polarization experiments showed that equilibration times were very short, i.e. just a few minutes, so that potentiokinetic measurements with 2V/h could be conducted without any particular errors. With anode polarization, the oxidation of the melt was accompanied by dissolution of the electrode material. With the metals Ni, Fe, Pt, and Au, covering layers formed and inhibited further dissolution [1]. On the other hand, Ag produced no covering layer [1] and, in agreement with Janz, Conte and Neuenschwander [13], who conducted similar studies between 600 and 900° C in the ternary eutectic melt $Li_2CO_3/Na_2CO_3/K_2CO_3$, dissolves with a current-dependent Faraday yield (Fig. 10 and 11).

Under dry oxygen or in peroxide-containing melts, an anode reaction already takes place at potentials between about -0.4 and 0 V. This may be oxidation of the peroxide in accordance with (2) (Fig. 13). With increasing oxygen content and thus decreasing peroxide content in the melt, limiting currents develop.

Under pure nitrogen, the depelopment of a limiting current is observed above + 0.1 V for the anode materials Pt, Fe, and Ni (Fig. 12). In this case, what is involved is probably not oxidation of peroxide residues in the melt, but instead oxidation of anode material. Evidence for this view is specifically the fact that for Pt, which showed the highest limiting current of all the anode materials investigated, the currents were poorly reproducible and fluctuations occurred. The latter were more distinct and had greater amplitudes under moist nitrogen (Fig. 14) and could be interpreted on the basis

of potentiostatic holding tests by the dissolution of platinum, induced by water vapor and disturbed by unstable covering-layer formation.

In the anode reaction above + 1.2 V, the reaction involved may be oxidation of the melt to oxygen in accordance with (16). In the electrochemical oxidation of the melt, the NaOH is immediately oxidized to oxygen by (16). A stepwise oxidation via peroxide does not occur, since first no evidence was found for anodic peroxide formation and second the oxidation of peroxide to oxygen takes place considerably in advance of the oxidation of hydroxide ions. Similar conditions were observed by Gerischer and Gerischer [15] in sulfuric acid containing H_2O_2. Small limiting currents were observed for the metals Pt, Fe, and Ni with cathode polarization under nitrogen (Fig. 12). Probably, what is happening here is the reduction of surface oxides -- suggested by the higher current for Fe -- or the reduction of peroxide residues in the melt. With platinum, limiting currents which rose as the peroxide content of the melt increase were observed, as found by Goret [7] (Fig. 13). The limiting current under N_2 with 10 vol-% O_2 was between those for 2.2 and 3.4 wt-% Na_2O_2, corresponding to 0.9 and 1.4 wt-% O_2^{2-}. However, since the peroxide content was less than 0.1 wt-% after the same premelting time of 2 h under O_2, it must be assumed that under nitrogen, not only is peroxide reduced in accordance with (3), but also oxygen is reduced in accord- /643
ance with (1). Under moist nitrogen, the development of limiting currents was observed from about -1.4 V in agreement with figures in the literature [5-7], which increased with rising water content (Fig. 14). In this case, the reduction

$$2\ H_2O + 2e^- = H_2 + 2\ OH^- \qquad (25)$$

may occur. The reduction of sodium ions in accordance with (27) or the reduction of hydroxide ions in accordance with (24) can be assumed for the current rise from about -1.8 V (Fig. 13 and 14). From Fig. 12, we can estimate the decomposition voltage, obtaining about 2 V in agreement with Goret [7].

By combining the cathode reaction equations (23) and (24) the anode reaction equation (16), the following overall reactions can be derived

(a) for (23), $NaOH = Na + \frac{1}{4} O_2 + \frac{1}{2} H_2O$, (26)

(b) for (24), $2\,NaOH = \frac{1}{4} O_2 + \frac{1}{2} H_2O + \frac{1}{2} H_2 + Na_2O$. (27)

Assuming an activity of unity for all reaction partners at 500° C, the decomposition voltage obtained from these equations is about 2.5 V for (26) and 2.0 V for (27). This result suggests that it is (24) and not (23) which describes the cathode reaction.

Electrochemical studies, in connection with previously reported corrosion tests [1], show that chemical processes and not electrochemical ones are rate-determining for the dissolution of metals and metal oxides in molten hydroxide. Chemical reaction of the melt with oxygen in the air forms peroxide, which is consumed in the corrosion reaction.

REFERENCES

1. A. Rahmel and H. J. Krüger, Werkstoffeu. Korros. 18, 193 (1967).

2. B. Neumann and E. Bergve, Z. Elektrochem. 20, 271 (1914).

3. J. N. Agar and F. B. Bowden, Proc. R. Soc. A169, 206 (1939).

4. K. H. Stern and J. K. Carlton, J. phys. Chem. 58, 965 (1954).

5. G. Kern, P. Degobert and O. Bloch, C.r. hebd. Séanc. Acad. Sci., Paris 256, 1500 (1963).

6. G. Kern and O. Bloch, C.r. hebd. Séanc. Acad. Sci., Paris 258, 5431 (1964).

7. J. Goret, Bull. Soc. chim. Fr. 12, 1074 (1964).

8. B. A. Rose, G. J. Davis and H. J. T. Ellingham, Trans. Faraday Soc. 41, 154 (1948).

9. J. N. Gregory and N. Hodge, Gt. Brit. Atomic Energy Res. Establ. C/R 2439, (1958).

10. H. Lux and T. Niedermaier, Z. anorg. allg. Chem. 285, 246 (1956).

11. H. Lux, R. Kuhn and T. Niedermaier, Z. anorg. allg. Chem. 298, 285 (1959).

12. K. H. Stern and J. K. Carlton, J. phys. Chem. 58, 965 (1954).

13. G. J. Janz, A. Conte and E. Neuenschwander, Corrosion 19, 292 (1963).

14. M. M. Popov and D. M. Ginsburg, J. gen. Chim. (USSR) 26, 1107 (1956).

15. R. Gerischer and H. Gerischer, Z. phys. Chem. N. F. 6, 178 (1956).